Magnetospheric Impulse Response for Many Levels of Geomagnetic Activity

L. F. Bargatze[1,2] and D. N. Baker

University of California, Los Alamos National Laboratory, New Mexico

R. L. McPherron[2]

Institute of Geophysics and Planetary Physics, University of California, Los Angeles

E. W. Hones, Jr.

University of California, Los Alamos National Laboratory, New Mexico

The temporal relationship between the solar wind and magnetospheric activity has been studied using 34 intervals of high time resolution IMP 8 solar wind data and the corresponding AL auroral activity index. The median values of the AL index for each interval were utilized to rank the intervals according to geomagnetic activity level. The linear prediction filtering technique was then applied to model magnetospheric response as measured by the AL index to the solar wind input function VB_s. The linear prediction filtering routine produces a filter of time-lagged response coefficients which estimates the most general linear relationship between the chosen input and output parameters of the magnetospheric system. It is found that the filters are composed of two response pulses speaking at time lags of 20 and 60 min. The amplitude of the 60-min pulse is the larger for moderate activity levels, while the 20-min pulse is the larger for strong activity levels. A possible interpretation is that the 20-min pulse represents magnetospheric activity driven directly by solar wind coupling and that the 60-min pulse represents magnetospheric activity driven by the release of energy previously stored in the magnetotail. If this interpretation is correct, the linear filtering results suggest that both the driven and the unloading models of magnetospheric response are inportant facets of a more comprehensive response model.

Introduction

A major unsolved problem of solar-terrestrial physics is understanding how solar wind mass, momentum, and energy couple into and subsequently flow through the magnetospheric system. Over the past decade, two phenomenological models have been presented to explain the temporal response of the magnetosphere to changes in solar wind energy input. These are the driven model [*Perreault and Akasofu*, 1978; *Akasofu*, 1979, 1980] and the energy storage-release or unloading model [*McPherron*, 1970; *McPherron et al.*, 1973; *Hones*, 1979; *Baker et al.*, 1979, 1981a]. In both models the energy transfer or coupling process begins when enhanced magnetic merging is initiated on the dayside magnetopause. The process ends when the energy is irreversibly dissipated by auroral particle precipitation, Joule heating in the ionosphere, or particle injection into the ring current and when energy is lost from the magnetosphere via plasmoid formation [*Hones et al.*, 1984]. However, the sequence of events following dayside merging and preceding energy dissipation is different for the two models.

In the driven model the magnetosphere responds directly to variations in the external solar wind conditions. In this model the time lag between solar wind energy input and enhanced geomagnetic activity depends only on the time scale required to convect the transferred energy from the energy-coupling region directly to the energy dissipation region. In the unloading model the magnetosphere responds to the increase of solar wind energy input by storing energy in the magnetotail as magnetic flux is eroded from the dayside and convected tailward. Later the stored energy is released impulsively from the magnetotail at expansion phase onset, adding to the energy dissipated via convection. In this case the time delay between energy input and dissipation depends not only upon the convection time scale of the magnetosphere but also upon the time scales of the processes which control the release of stored energy from the magnetotail.

After two decades of study, no magnetospheric response model has been proposed which can successfully describe all observations. For instance, the energy storage-release model fails to account for events which show a clear onset of substorm activity without an accompanying decrease in the tail lobe magnetic flux density [*Akasofu*, 1980; *Kan et al.*, 1980]. Similarly, the driven model cannot account for geomagnetic activity which occurs long after the last interval of enhanced solar wind energy input.

Recently, the comparison of magnetospheric response models has been greatly aided by the technique of linear prediction filtering [*Iyemori et al.*, 1979; *Iyemori and Maeda*, 1980; *Clauer et al.*, 1981, 1983]. This method uses a filter [*Wiener*, 1949; *Levinson*, 1949] to model the most general, linear relationship between measured magnetospheric and solar wind quantities. Once found, the filter $H(t)$ may be used along with the solar wind input time series $I(T)$ to estimate the solar wind driven component of geomagnetic activity $O(T)$ via the convolution theorem:

$$O(T) = \int_0^\infty H(t)I(t-T)\,dt \tag{1}$$

where T is the time of observation and t is the time lag.

---

[1] Also at Institute of Geophysics and Planetary Physics, University of California, Los Angeles.
[2] Also at Department of Earth and Space Sciences, University of California, Los Angeles.

Clauer et al. [1981] used the solar wind inputs VB_s, V^2B_s, and ε along with the linear filtering routines to model the response of the *AL* and *AU* indices to solar wind variations. The *AL* and *AU* indices are auroral geomagnetic activity indices which are roughly proportional to the Joule heating rate of the westward and eastward electrojets, respectively [*Perreault and Akasofu*, 1978]. The parameter $\varepsilon = VB^2l_0^2 \sin^4 (\theta/2)$ is a solar wind coupling function [*Akasofu*, 1979] which has been identified as the dynamo power delivered from the solar wind to the open magnetosphere [*Kan and Lee*, 1979; *Kan et al.*, 1980]. In the formulas above, V is the solar wind bulk speed, and $B_s = -B_z$ for $B_z < 0$ and $B_s = 0$ for $B_z > 0$, where the interplanetary magnetic field (IMF) is expressed in geocentric solar magnetospheric (GSM) coordinates. *Clauer et al.* [1981] found that the VB_s, V^2B_s, and ε time series alone can predict only about 40% of the *AL* index variance and less of the *AU* index variance. They conclude that the remaining *AL* and *AU* index variance is not modeled because either the chosen solar wind input time series are not proper estimates of the actual solar wind input or the remaining variance is simply not related to the time-varying solar wind conditions. *Clauer et al.* [1981] also found that the time lag to peak filter amplitude is smaller for substorms of large magnitude than for substorms of small magnitude. Further, they suggest that the response of the magnetosphere is not completely linear; otherwise, the filter properties would not vary with the magnitude or level of geomagnetic activity.

In this paper we extend the study of *Clauer et al.* [1981] and determine how the properties of the solar wind–*AL* index response filter vary with the overall level of geomagnetic activity. To do this, we have used a new and larger data set and a novel method to organize the data with respect to geomagnetic activity level. Only then are the data input to the linear filtering routines.

DATA

The data set used in this study contain the *AL* index and solar wind plasma and IMF measurements at 2.5-min time resolution. The solar wind data are from IMP 8, which was launched in late October 1973 into an elliptical, 23 × 46 R_E, orbit. The original IMP 8 plasma and IMF observations were averaged over 2.5-min periods for comparison with *AL* index values. The *AL* index values were obtained from the World Data Center, Boulder, Colorado. The data set spans the interval from November 1973 to December 1974 and is the same data set used by *Baker et al.* [1981b] to study the correlation of the *AE* index with interplanetary parameters.

The IMF data and the IMP 8 ephemeris data we have utilized are expressed in geocentric solar magnetospheric (GSM) coordinates. The GSM coordinate system is useful in studying solar wind–magnetosphere interactions, since it reduces the three-dimensional motion of the earth's dipole to motion in the GSM *X-Z* plane [*Russell*, 1971].

For the present study the ideal position to monitor solar wind conditions is at a point just upstream of the merging region where energy enters the magnetosphere from the solar wind. This situation rarely occurs with IMP 8. Consequently, one must modify the solar wind time series to account for the change in time delay between corresponding events occurring at IMP 8 and the coupling region. To do this, we have estimated the actual time delay using a formula developed by Zwickl and coworkers [cf. *Baker et al.*, 1983]. Here, the for-

mula has been expressed ignoring the orbital motion of the earth and using a small-angle approximation:

$$t(V, X, Y) = \frac{X - X_0}{V} - (Y - Y_0)\frac{T_0}{2\pi a} \qquad (2)$$

where

t model solar wind time delay;

X, Y IMP 8 position in GSM coordinates;

X_0, Y_0 nominal coupling region coordinates, with $(X_0, Y_0) = (15\ R_E, 0\ R_E)$;

V instantaneous solar wind bulk speed;

T_0 mean solar rotation period;

a mean radius of earth's orbit about the sun.

The first term of the formula accounts for the radial motion of plasma convecting at the solar wind speed, while the second term accounts for azimuthal drift of plasma due to solar rotation. It was found that time shifts of 10 min occur frequently for typical solar wind conditions and IMP 8 positions. Even larger time delays are found when solar wind speeds are small and when IMP 8 was far upstream or downstream from the merging region.

The solar wind propagation delay model implicitly assumes that (1) solar wind conditions are spatially uniform over a few tens of R_E, (2) the position of the coupling region does not vary with time, and (3) solar wind discontinuities or transients are parallel to phase fronts, where phase fronts are planes in the solar wind which have constant model time delay.

The first assumption is usually satisfied [*Russell et al.*, 1980; *Crooker et al.*, 1982]. However, the position of the coupling region can change if the IMF orientation [*Crooker et al.*, 1979; *Luhmann et al.*, 1984] or the solar wind dynamic pressure varies. Further, the relative orientation between a solar wind phase front and a solar wind discontinuity changes with time and is not always well constrained by observations. Despite these complications it is found that the *AL* index modeling efficiency is increased whenever time-shifted solar wind data were used as input to the analysis.

The routines used to estimate the model filters in this study cannot accept missing data in either the input $I(T)$ or the output $O(T)$ time series. The *AL* index data set is complete, but unfortunately, the solar wind plasma and IMF data sets are not. For periods of about 6 days each orbit, IMP 8 did not monitor solar wind conditions because it was within the earth's magnetosphere. Also, there are numerous data gaps which occur randomly throughout the solar wind data set, which last anywhere from 2.5 min to several hours.

The data gaps which occur whenever IMP 8 leaves the solar wind are too long to be interpolated and used as input to model geomagnetic activity. This is because the solar wind input calculations are sensitive to interpolation across time gaps longer than the time scale over which solar wind conditions vary. Hence we were forced to inspect separately the data from each IMP 8 solar wind pass to find events suitable for study.

The solar wind data set was scanned to compile a list of data intervals, which are defined as any segment of data which is at least 1 day long with less than 10% data gaps. The initial list contained roughly 30 intervals with time lengths between 1 day and 4 days long. Then, the data gaps in these intervals were interpolated linearly to satisfy the modeling routine restrictions. More than 95% of the data gaps were shorter than 10 min.

The data interval list was then modified on the basis of three criteria:

1. A data interval must be temporally bounded at both ends by a 2-hour segment of small, nearly zero solar wind input and *AL* index values.

2. A data interval can contain a multiple number of auroral zone events if, and only if, the events have roughly the same *AL* index magnitudes.

3. A data interval must be split into two or more data intervals if it includes two or more daylong segments which independently satisfy the first two criteria.

Enforcing the first criterion allows us to use concatenated data intervals as input to the modeling routines. Otherwise, fallacious time lags between solar wind and auroral time series on opposite sides of a splice would contaminate the results. The second and third criteria aid us later, when we attempt to sort the list of data intervals according to "activity level."

At this point an intermediate list of data intervals was obtained with a total of 34 intervals. In all the intervals contain 73 days of data, which corresponds to about one third of the original IMP 8 solar wind data.

Next, we calculated the integral occurrence percentages of the *AL* index for each data interval; these are plotted in Figure 1. Consider first the rightmost curve in Figure 1. About 75% of the *AL* index values in this interval were below -100 nT and 50% of the *AL* values were below -180 nT. In comparison, the next curve to the left reaches the same occurrence fractions at smaller *AL* values near -70 and -170 nT. Evidently, the rightmost curve corresponds to a data interval which is relatively more active than the data interval corresponding to the second curve.

By examining Figure 1 closely, one notices that the integral occurrence histograms maintain nearly the same order for all occurrence percentages. Thus we were free to choose the 50% integral occurrence value of the *AL* index to assess the geomagnetic "activity level" in each data interval. We then spliced the data intervals end-to-end in the order of increasing activity level to generate the analysis data set.

ANALYSIS AND RESULTS

Each set of five consecutive data intervals in the analysis data set was used as input to the prediction routines to estimate the empirical response of the magnetosphere relating the
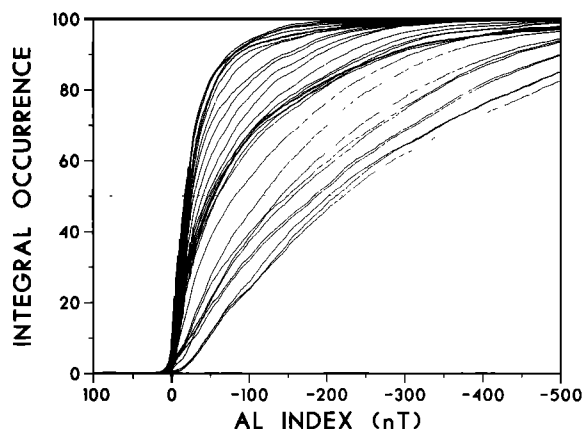
Fig. 1. Integral occurrence percentages of the *AL* index for 34 data intervals. Each occurrence percentage curve corresponds to a single data interval. The 50% occurrence percentage was utilized to assess the geomagnetic "activity level" in each data interval.
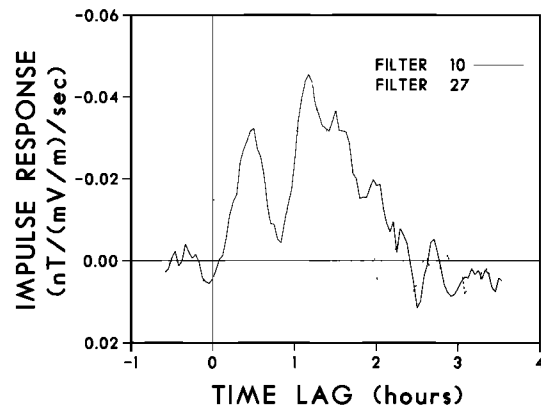
Fig. 2. A plot of filter 10 and filter 27. These filters correspond to moderately and strongly active data intervals, respectively. The vertical axis is plotted using the units of the *AL* index (in nanoteslas) divided by units of the solar wind electric field (in millivolts per meter) and normalized by the data sampling period (150 s).

AL index to the solar wind input VB_s. Since there are 34 data intervals in the data set, 30 filters numbered from 1 to 30 in order of increasing overall geomagnetic activity level were obtained. Two of these filters 10 and 27, are plotted in Figure 2. Filter 27 was generated using very active data intervals with *AL* index median values near -150 nT. In contrast, filter 10 was generated using moderately active data intervals with *AL* index median values near -50 nT. Both of these filters possess a response pulse which rises from near zero at zero time lag, peaks near 20-min time lag, and decays thereafter. Filter 10 has a second response pulse which peaks at a lag of 60 min and decays to zero after about 2.5-hour time lag. Filter 27 suggests the presence of a second pulse, but its signature is dominated by that of the first pulse.

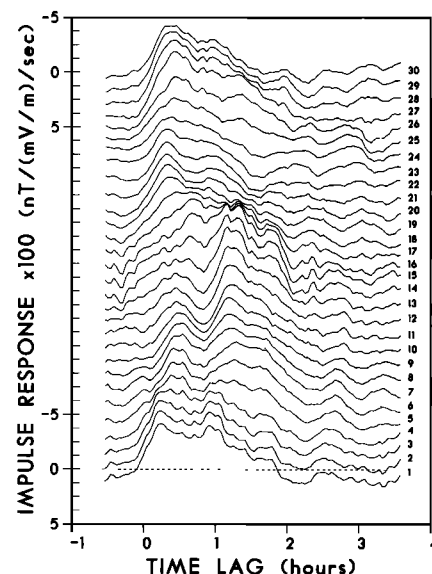Figure 3 is a stack plot of all filters arranged in order of

Fig. 3. A stack plot of linear prediction filters for all levels of geomagnetic activity. The geomagnetic "activity level," based on the distributions in Figure 1, increases unevenly from filter 1 through 30. A dashed baseline and a vertical scale are included for filter 1, and a vertical scale is included for filter 30. Each successive filter is plotted after a cumulative, vertical displacement of one tick mark. Note that the filter coefficients were multiplied by 100 before plotting.

increasing geomagnetic activity level (activity index) from bottom to top. Note that the filters labeled from 1 to 18 have two response pulses. For filters 6–18 the pulse peaking near 60-min time lag has a larger amplitude than the pulse peaking near 20 min. The two pulses have roughly the same amplitude for filters 1–5. Filters 19–30 each possess a response pulse which reaches a maximum amplitude near 20-min lag and decays thereafter, just as outlined for filter 27. The two pulses shall be referred to by using the respective time lags to maximum amplitudes: 20 and 60 min. However, note that there is some variability in these time lags: from about 15 to 30 min for the first pulse and about 55 to 70 min for the second pulse. Some of this variation is purely statistical, but some may be due to systematic errors in time shifting the solar wind data, and another fraction could represent real variability in response time of the magnetosphere.

Figure 4 is a plot of the input and output time series for two 5-day intervals. The top set of three panels shows data used to calculate filter 10; the bottom set of three panels shows data used to calculate filter 27. Within each set the VB_s input is plotted in the top panel, the original and the predicted AL index output are plotted in the middle panel, and the residual AL index is plotted in the bottom panel. The predicted AL index is calculate utilizing the VB_s input, the empirical filter, and the convolution equation. Note that the predicted AL index is the more smoothly varying curve plotted in the middle panels. Also, the residual AL index is equal to the difference of the original and the predicted AL index.

The predicted AL index corresponds to the portion of the observed AL index which is time correlated with solar wind (VB_s) variations. The residual AL index corresponds to the portion of the observed AL index which is not time correlated with solar wind variations. In this light, several observations become evident upon comparing the time series in Figure 4. First, both the VB_s time series and the residual AL index time series have a high-frequency component. However, these high-frequency components are not correlated. This implies that the magnetosphere behaves like a low-pass filter of solar wind variations [Clauer et al., 1981]. Second, the residual AL index time series contains sharp, negative deviations which do not resemble noise. Instead, these features appear to be the signatures of substorms which are not predictable using only solar wind data. The residual AL index time series also contains intervals of slowly varying, positive deviations. It is not understood why the AL index is overpredicted during these intervals. In agreement with Clauer et al. [1983] we find that about 45% of the AL index variance can be modeled using the linear prediction filtering technique. The prediction efficiency does not seem to vary with the level of geomagnetic activity.

DISCUSSION AND CONCLUSIONS

An important result of this study is that the VB_s to AL response filters peak at a time lag near 20 min for intervals of strong geomagnetic activity, while the moderate activity filters peak at a time lag near 60 min. Clauer et al. [1981] obtained filters with nearly identical features by studying two 10-day intervals, one of which contained periods of very strong geomagnetic activity, while the other contained more moderate activity. They suggested that the filters were best described as a single pulse which peaked at shorter time lags for more active intervals. Using a larger data set organized by geomagnetic activity level, we find that the filters are better described as the superposition of two pulses which peak near 20 and 60 min. Furthermore, we find that the difference between strong

and moderate (or weak) activity filters can be explained by a change in the relative magnitude of the two pulses.

It might be questioned whether the two peaks in the VB_s to AL filters are significant and reproducible. We believe that these peaks are indeed significant and reproducible for three reasons:

1. The two peaks are present in the moderate activity, VB_s to AL filter plotted in Figure 2 of Clauer et al. [1981]; this filter was generated independently by using an Explorer 33 data set.
2. The two peaks are clearly seen in each of the filters from 1 to 18, even though every fifth filter was generated using an entirely separate set of data intervals.
3. The amplitude of the statistical fluctuation in the filter estimates is small with respect to the amplitude of the two peaks.

We also tested other input and output combinations such as VB_s to AE, ε to AL, and ε to AE and found that these filters possess the same features described for the VB_s to AL filters.

It is interesting to compare the present results to those of Baker et al. [1981b], who utilized the same data set to perform a high time resolution cross-correlation analysis between the AE index and VB_s. They found that VB_s to AE correlation values maximize at a time lag near 40 min. Our VB_s to AL filters reach a peak lag near to either 20 or 60 min, depending on activity level. Given that AL is a substantial component of AE, we would expect on the average that the filters would peak near the cross-correlation lag of 40 min if the data set studied included an equal number of weakly, moderately, and strongly active data intervals.

A possible interpretation of the present results is that the pulses peaking near 20 and 60 min each correspond to a separate response mode of the magnetosphere. Further, as discussed below, it is possible that the 20-min pulse corresponds to electrojet activity related to direct interaction between the solar wind and the magnetosphere, while the 60-min pulse corresponds to electrojet activity due to the release of stored electromagnetic energy from the tail. If this is true, then the differences between strong and moderate activity filters can be explained by a change in the relative importance of the solar wind driven and tail release components of magnetospheric activity.

There is other support for the interpretation made above. For example, Meng [1979] found that the motion of the midday auroral oval can be modeled using B_z variations and an equation with an exponential time constant of about 17 min. Also, Holzer and Reid [1975] and Reid and Holzer [1975] found that the time constant for the magnetosphere-ionosphere system to become adjusted to a change in the dayside reconnection rate is about 20 min. Their conclusion is based upon applying a circuit analog for the dayside magnetosphere-ionosphere system to real observations of a magnetopause erosion event. They suggest that the time constant is related to the time required for the ionospheric convection pattern to change in response to the variation of the solar wind boundary conditions. These studies suggest that the convection of plasma within the magnetosphere responds to the solar wind over a time scale near the 20-min time lag found for the first response pulse of the VB_s to AL filters. If this comparison is valid, then the results of this study imply that solar wind control of magnetospheric convection is important for all levels of geomagnetic activity. In this sense, the dependence of the 20-min pulse amplitude upon the level of geomagnetic activity (see Figure 3) indicates that the solar
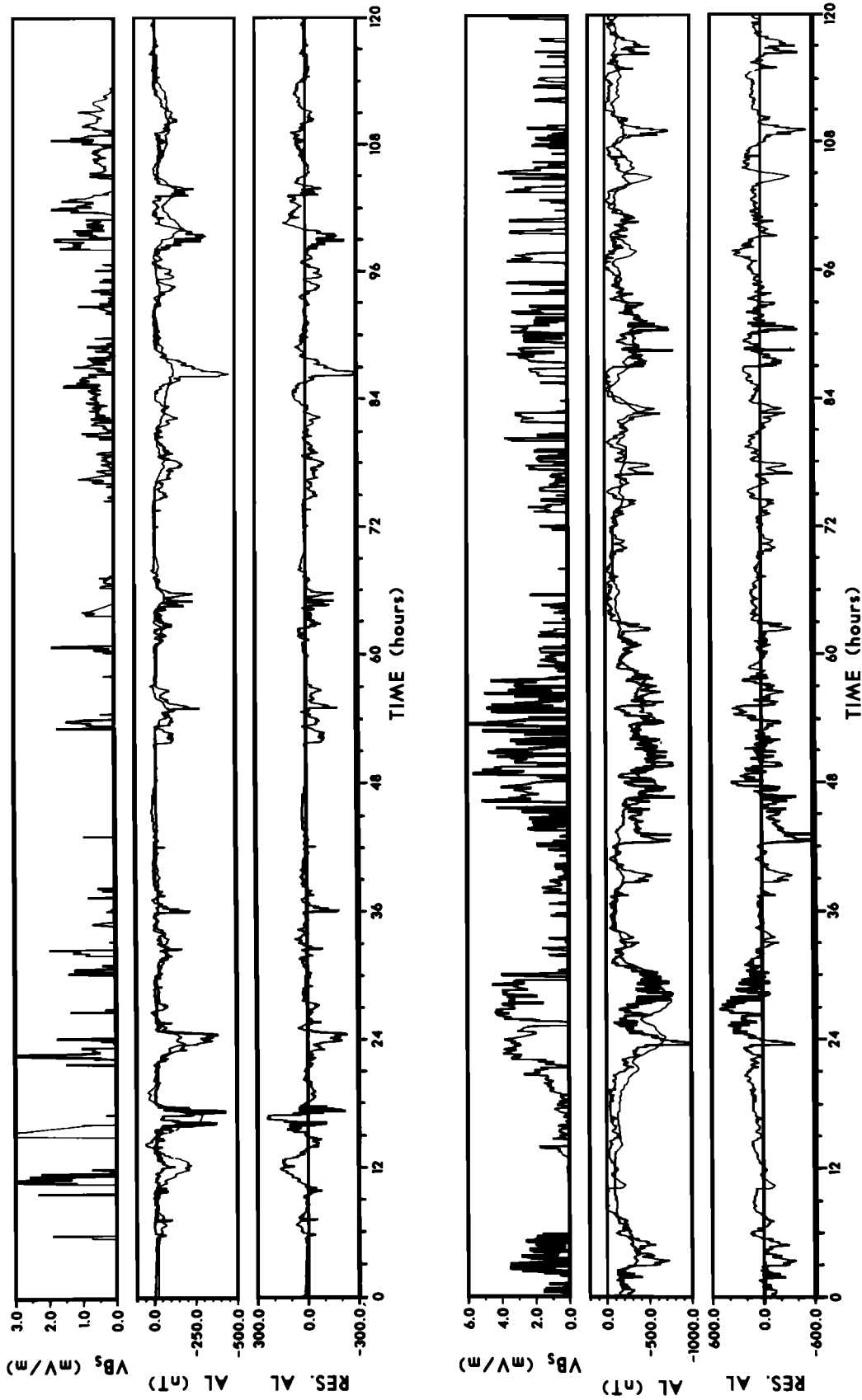
Fig. 4. A plot of the VB_s, original AL index, predicted AL index, and residual AL index time series for moderate (top three panels) and strong (bottom three panels) geomagnetic activity levels. The moderate and strong activity data shown here correspond to a 5-day subset of the data used to calculate filter 10 and filter 27. Note that the predicted AL index time series is the more smoothly varying function plotted in the middle panel of each set of panels.
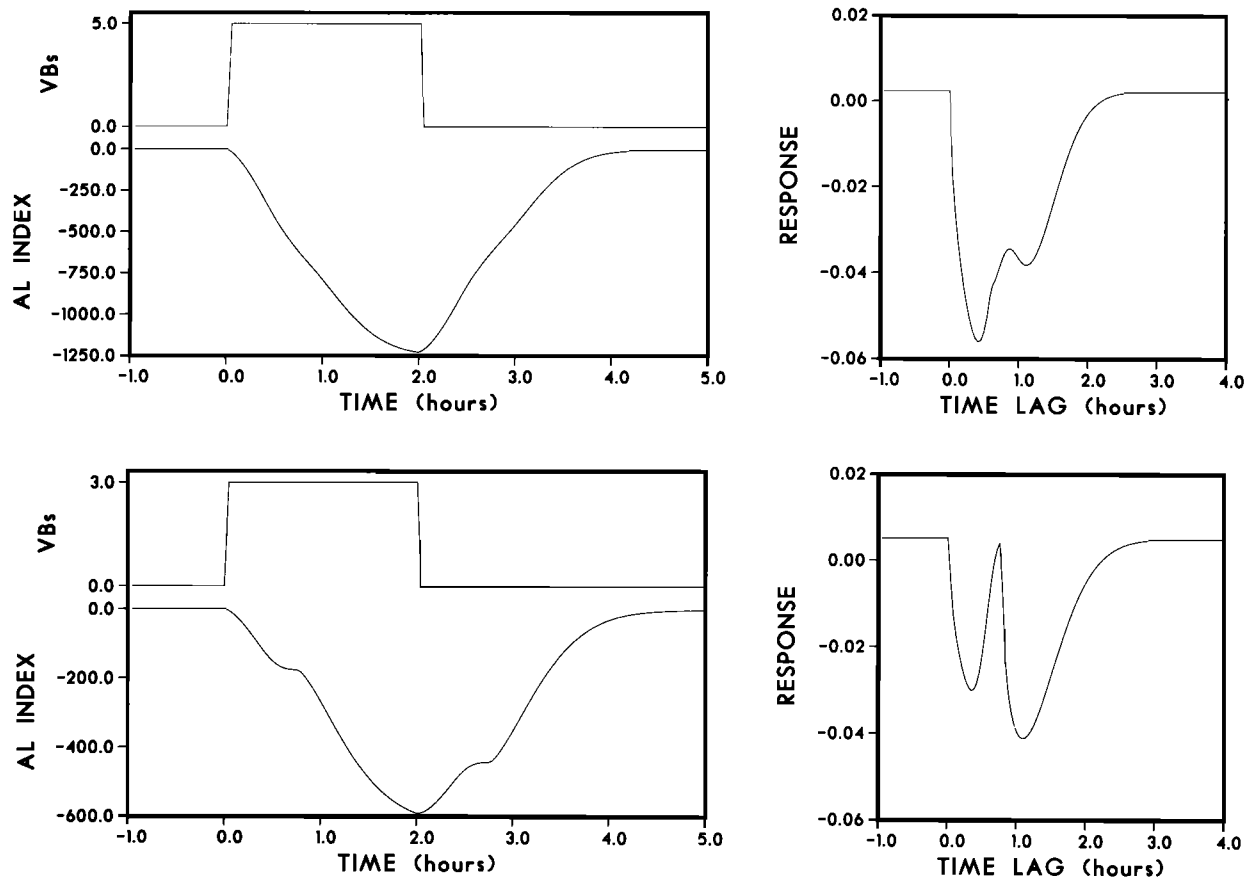
Fig. 5.   Examples of model response filters, VB_s input time series and AL index output time series for strong geomagnetic activity (top panels) and moderate geomagnetic activity (bottom panels).

wind control of magnetospheric convection is most efficient for intervals of strong activity.

Iyemori [1980] found that the time delay between the southward turning of the IMF and the onset of a substorm was near 1 hour, with a range of 0.75 to 1.25 hours. Of course, many correlative studies [i.e., *Foster et al.*, 1971; *Baker et al.*, 1981b] find a similar time lag. Some researchers have suggested that the 1-hour lag corresponds to the substorm growth phase during which solar wind energy is convected from the dayside merging region into the tail, where it is stored in the form of increased magnetic energy density [*McPherron*, 1970]. Recall that 1 hour corresponds closely with the time delay of the second pulse in the filters. If this correspondence is correct, then the storage of energy in the tail with sudden release of this energy on a time scale of ~ 1 hour is the dominant magnetospheric response mode for moderately active time intervals.

In Figure 5 we demonstrate the significance of the differences between the moderate and strong activity filters in the time domain. The top two panels are for strong activity. In the top right panel we plot a model filter created by fitting a simple analytical function to the strong activity filter 27. This analytical function was then convolved with a 5 mV/m, square wave VB_s input of a 2-hour duration to create a sample AL index time series. The VB_s and AL index time series are plotted in the top left panel. Similarly, in the lower panels of Figure 5 an analytical function was fitted to filter 10, which was then convolved with a 3 mV/m, square wave VB_s input to produce a sample moderate activity AL index time series.

For strong activity (top panels) the AL index decreases monotonically from zero at the start of the square wave input to -1250 nT after 2 hours. By this time, nearly the whole filter has been "activated," and the AL index has almost reached what would be its saturation value for the given input amplitude. The AL index begins to increase as soon as VB_s goes to zero or, equivalently, as the IMF turns northward. Two hours after energy input has ceased, the AL index values have returned to zero. For this example the effects of the second response pulse are subtly expressed as slope changes in the AL index time series.

For moderate activity the AL index time series is more interesting. At first, for about 30 min the index begins to decrease, but it then levels off near a value of -180 nT after about 45 min. As the second pulse of the moderate activity filter is activated, the AL index decreases more rapidly, reaching a value of -600 nT. The index then increases as the VB_s input goes to zero and then increases more quickly as the second pulse of the filter becomes deactivated. Again, the AL index reaches zero about 4 hours after the input started and 2 hours after input stopped.

For moderate activity, 180 nT of the 600 nT maximum AL index magnitude is provided by the first pulse of the response filter. This means that only 30% of the AL index variation is due to the driven mode of magnetospheric response. For strong activity, more than half of the AL index variation is due to the driven component of response. However, one must be careful in equating the percentage of AL index variance to the relative amount of energy dissipated by the driven and

unloading systems. Indeed, one must exercise caution in using the auroral indices to study substorms. Rostoker [1972] suggested that well-defined, localized substorms may be ignored in the auroral indices if the substorm current systems are localized or if the electrojet is displaced well poleward or equatorward of the magnetic observatories used to compute the indices. Allen and Kroehl [1975] reported that the indices are also contaminated by errors due to unequal local time spacing of the magnetic observatories. Also, the auroral indices may register a lower limit to the total ionospheric current flow due to the sparse local time and latitudinal spacing of the observatories [Rostoker et al., 1980]. Furthermore, Akasofu and Ahn [1972] suggested that the AE index ($AE = AU - AL$) is less accurate for values of the index smaller than about 250 nT. Some better measure such as the total current flow in the electrojets should be used to quantify the absolute energy dissipation rates of the driven and unloading systems.

It is tempting to identify the initial 45-min period as the growth phase of the substorm followed by the expansion phase and then by the recovery phase. The time of expansion phase onset is determined by the activation of the moderate filter's second pulse, and the onset of recovery is coincident with the northward turning of the IMF. The "decay" phase which begins at the onset of recovery could represent the decrease of currents flowing in the convection-driven system. Note that it is difficult to identify the growth phase for the strong activity AL index example. This is due to the mostly unimodal response character of the magnetosphere for strong activity levels. Comparison of the two AL index time series reveals the quicker increase and decrease of the index for stronger activity levels.

While these examples certainly reveal many observed features of AL index variations, they do not show the sudden and large fluctuations that are often present at expansion phase onset. However, such variations occur in a somewhat random fashion in time, magnitude, and duration. The examples plotted in Figure 5 must be seen as simple examples that show the time variations of the AL index in a statistical, average way.

In summary, we have shown that the response of the magnetosphere for VB_s to AL is not completely linear. We have focused on this feature using a new and larger data set and a novel method for organizing the data set according to the level of geomagnetic activity. Our empirical results indicate that the magnetosphere responds more quickly for data intervals with higher levels of activity. A second interesting result is that the VB_s to AL response filter is composed of two pulses peaking at different time lags. The first pulse peaks at 20-min lag and is dominant for strongly active intervals, while the second pulse peaks at 60-min lag and is the dominant pulse for moderately active intervals. Further, this linear filtering analysis has provided new insight into old models of solar wind–magnetosphere coupling. Both the driven and energy storage-release models of magnetospheric response can be seen as facets of a more comprehensive model.

The Editor thanks the two referees for their assistance in evaluating this paper.

REFERENCES

Akasofu, S.-I., Interplanetary energy flux associated with magnetospheric substorms, *Planet. Space Sci., 27*, 425, 1979.

Akasofu, S.-I., The solar wind-magnetosphere energy coupling and magnetospheric disturbances, *Planet. Space Sci., 28*, 495, 1980.

Akasofu, S.-I., and B.-H. Ahn, Magnetospheric convection at a low level power ε, *Planet. Space Sci., 30*, 1057, 1982.

Allen, J. H., and H. W. Kroehl, Spatial and temporal distributions of magnetic effects of auroral electrojets as derived from AE indices, *J. Geophys. Res., 80*, 3667, 1975.

Baker, D. N., R. D. Belian, P. R. Higbie, and E. W. Hones, Jr., High-energy magnetospheric protons and their dependence on geomagnetic and interplanetary conditions, *J. Geophys. Res., 84*, 7138, 1979.

Baker, D. N., E. W. Hones, Jr., P. R. Higbie, R. D. Belian, and P. Stauning, Global properties of the magnetosphere during a substorm growth phase: A case study, *J. Geophys. Res., 86*, 8941, 1981a.

Baker, D. N., E. W. Hones, Jr., J. B. Payne, and W. C. Feldman, A high time resolution study of the interplanetary parameter correlations with AE, *Geophys. Res. Lett., 8*, 179, 1981b.

Baker, D. N., R. D. Zwickl, S. J. Bame, E. W. Hones, Jr., B. T. Tsurutani, E. J. Smith, and S.-I. Akasofu, An ISEE 3 high time resolution study of interplanetary parameter correlations with magnetospheric activity, *J. Geophys. Res., 88*, 6230, 1983.

Clauer, C. R., R. L. McPherron, C. Searls, and M. G. Kivelson, Solar wind control of auroral zone geomagnetic activity, *Geophys. Res. Lett., 8*, 915, 1981.

Clauer, C. R., R. L. McPherron, and C. Searls, Solar wind control of the low-latitude asymmetric magnetic disturbance field, *J. Geophys. Res., 88*, 2123, 1983.

Crooker, N. U., Dayside merging and cusp geometry, *J. Geophys. Res., 84*, 951, 1979.

Crooker, N. U., G. L. Siscoe, C. T. Russell, and E. J. Smith, Factors controlling degree of correlation between ISEE 1 and ISEE 3 interplanetary magnetic field measurements, *J. Geophys. Res., 87*, 2224, 1982.

Foster, J. C., D. H. Fairfield, K. W. Ogilvie, and T. J. Rosenberg, Relationship of interplanetary parameters and occurrence of magnetospheric substorms, *J. Geophys. Res., 76*, 6971, 1971.

Holzer, T. E., and G. C. Reid, The response of the dayside magnetosphere-ionosphere system to time-varying field line reconnection at the magnetopause, 1, Theoretical model, *J. Geophys. Res., 80*, 2041, 1975.

Hones, E. W., Jr., Transient phenomena in the magnetotail and their relation to substorms, *Space Sci. Rev., 23*, 393, 1979.

Hones, E. W., Jr., D. N. Baker, S. J. Bame, W. C. Feldman, J. T. Gosling, D. J. McComas, R. D. Zwickl, J. Slavin, E. J. Smith, and B. T. Tsurutani, Structure of the magnetotail at 220 R_E and its response to geomagnetic activity, *Geophys. Res. Lett., 11*, 5, 1984.

Iyemori, T., Time delay of the substorm onset from the IMF southward turning, *J. Geomagn. Geoelectr., 32*, 267, 1980.

Iyemori, T., and H. Maeda, Prediction of geomagnetic activity from solar wind parameters based on the linear prediction theory, in *Solar-Terrestrial Predictions Proceedings*, edited by R. F. Donnelly, vol. 4, p. A-1, National Oceanic and Atmospheric Administration, Boulder, Colo., 1980.

Iyemori, T., H. Maeda, and T. Kamei, Impulse response of geomagnetic indices to interplanetary magnetic field, *J. Geomagn. Geoelectr., 31*, 1, 1979.

Kan, J. R., and L. C. Lee, Energy coupling function and solar wind-magnetosphere dynamo, *Geophys. Res. Lett., 6*, 577, 1979.

Kan, J. R., L. C. Lee, and S.-I. Akasofu, The energy coupling function and the power generated by the solar wind-magnetosphere dynamo, *Planet. Space Sci., 28*, 823, 1980.

Levinson, N., The Wiener RMS (root-mean-square) error criterion in filter design and prediction, Appendix B, in *Extrapolation, Interpolation, and Smoothing of Stationary Time Series with Engineering Applications*, edited by N. Wiener, John Wiley, New York, 1949.

Luhmann, J. G., R. J. Walker, C. T. Russell, N. U. Crooker, J. R. Spreiter, S. S. Stahara, and D. J. Williams, Mapping the magnetosheath field between the magnetopause and the bow shock: Implications for magnetospheric particle leakage. *J. Geophys. Res., 89*, 6829, 1984.

McPherron, R. L., Growth phase of magnetospheric substorms, *J. Geophys. Res., 28*, 5592, 1970.

McPherron, R. L., C. T. Russell, and M. P. Aubry, Satellite studies of magnetospheric substorms on August 15, 1968, 9, Phenomenological model for substorms, *J. Geophys. Res., 78*, 3131, 1973.

Meng, C.-I., Polar cap variations and the interplanetary magnetic field, in *Dynamics of the Magnetosphere*, edited by S.-I. Akasofu, p. 23, D. Reidel, Hingham, Mass., 1979.

Perreault, P., and S.-I. Akasofu, A study of geomagnetic storms, *Geophys. J. R. Astron. Soc., 54*, 547, 1978.

Reid, G. C., and T. E. Holzer, The response of the dayside magnetosphere-ionosphere system to time-varying field line reconnection at the magnetopause, 2, Erosion event of March 27, 1968, *J. Geophys. Res., 80*, 2050, 1975.

Rostoker, G., Geomagnetic indices, *Rev. Geophys., 10*, 935, 1972.

Rostoker, G., S.-I. Akasofu, J. Foster, R. A. Greenwald, Y. Kamide, K. Kawasaki, A. T. Y. Lui, R. L. McPherron, and C. T. Russell, Magnetospheric substorms—Definitions and signatures, *J. Geophys. Res., 85*, 1663, 1980.

Russell, C. T., Geophysical coordinate transformations, in *Cosmic Electrodyn., 2*, 184, 1971.

Russell, C. T., G. L. Siscoe, and E. J. Smith, Comparison of ISEE 1 and 3 interplanetary magnetic field observations, *Geophys. Res. Lett., 7*, 381, 1980.

Wiener, N. (Ed.), *Extrapolation, Interpolation, and Smoothing of Stationary Time Series with Engineering Applications*, John Wiley, New York, 1949.

D. N. Baker, L. F. Bargatze, and E. W. Hones, Jr., Los Alamos National Laboratory, ESS-8 D438, Los Alamos, NM 87545.

R. L. McPherron, Institute of Geophysics and Planetary Physics, University of California, Los Angeles, CA 90024.